Rotating Molten Metallic Drops and Related Phenomena: A New Approach to the Surface Tension Measurement

Won-Kyu Rhim and Takehiko Ishikawa[*]

Jet Propulsion Laboratory, California Institute of Technology, M/S 183-401,
4800 Oak Grove Drive, Pasadena, California 91109, USA
Tel: (818) 354-2925, FAX: (818) 393-5039
e-mail: won-kyu.rhim@jpl.nasa.gov

*On leave from the National Space Development Agency of Japan

Abstract

Molten aluminum and tin drops were levitated in a high vacuum by controlled electric fields, and they were systematically rotated by applying by a rotating magnetic field. When the evolution of the drop shape was measured as a function of rotation frequency, it agreed quantitatively well with the Brown and Scriven's theoretical prediction. The normalized rotation frequencies at the bifurcation point agreed with the predicted value 0.559, within 2%.

An anomalous phenomenon which totally deviated from the prediction was observed in rotating molten tin drops when they were kept in a high rotation rate for several hours. No anomaly was observed in aluminum drops when they underwent similar condition. It was speculated that under the strong centrifugal force in the drop the tin isotopes must be separating. Since ^{27}Al is essentially the only naturally abundant isotope in the aluminum drops, the same anomaly is not expected.

Based on the shape deformation of a rotating drop, an alternate approach to the surface tension measurement was verified. This new surface tension measurement technique was applied to a glassforming alloy, $Zr_{41.2}Ti_{13.8}Cu_{12.5}Ni_{10.0}Be_{22.5}$ in its highly viscous states.

Also demonstrated in the paper was a use of a molten aluminum drop to verify the Busse's prediction of the influence of the drop rotation on the drop oscillation frequency.

1. Introduction

Since Rayleigh's[1] initial calculation of axi-symmetric shapes of rotating drops, the theoretical predictions of drop rotaion processes have been brought to a rare degree of accuracy by Chandrasekhar[2], and more recently by Brown and Scriven[3]. Over the last decade there have been several efforts to experimentally verify these predictions. Rhim, Chung, and Elleman[4] performed an experiment in a ground-based laboratory using a charged water drop suspended by an electrostatic levitator. They rotated the drop exerting an acoustic torque, and observed the bifurcation occurring very close to the theoretical prediction. However, the drop which carried electric charges on its surface cast some doubts as a valid system for the verification of the theory which assumed electrically neutral drops. Biswas, Leung, and Trinh[5] studied a rotating drop which was acoustically levitated in a ground-based laboratory. Using an initially deformed drop (in static state), they obtained results which could expain the anomaly that was observed during the 1986 Spacelab experiments[6]. Recently Wang, Anilkumar, Lee, and Lin[7] repeated their experiment with improved equipment in the Space Shuttle (USML-1). Using spherical drops of silicone oil and glycerin/water mixture, they obtained results that closely agreed with the theoretical prediction when the drops rotated, satisfying the solid-body-rotation condition. All the above experiments were conducted in ambient conditions where air friction could have prevented the drops from satisfying a perfect solid-body rotation condition.

In this paper a new way of studying drop dynamics using molten metallic drops will be described as it was was applied in various experiments. Since a molten drop rotates in a frictionless environment of high vacuum, in absence of an applied torque, a drop will continue rotating almost indefinitely, eventually reaching a true solid-body rotation state due to the viscosity. This capability is demonstrated as it is applied in the following experiments: (i) the verification of Brown-Scriven's theory on the drop-shape evolution during the solid-body-rotation, (ii) the deviation from the prediction that was observed in rotating tin drops, (iii) a new way of measuring surface tension based on the drop rotation, and its application to a

highly viscous glassforming alloy, and (iv) the verification of Busse's prediction on the oscillation of a rotating drop.

2. Experimental Apparatus and Approach

The basic principle of the sample rotation was based on the application of steady (or step-by-step) low-level torque to a molten metallic drop that was levitated in a high vacuum. The High Temperature Electrostatic Levitator (HTESL) at Jet Propulsion Laboratory levitates a sample about 3 mm in diameter between a pair of parallel disk electrodes that are spaced about 12 mm (Fig. 1). The electric field between these two electrodes produce strong electrostatic force on a
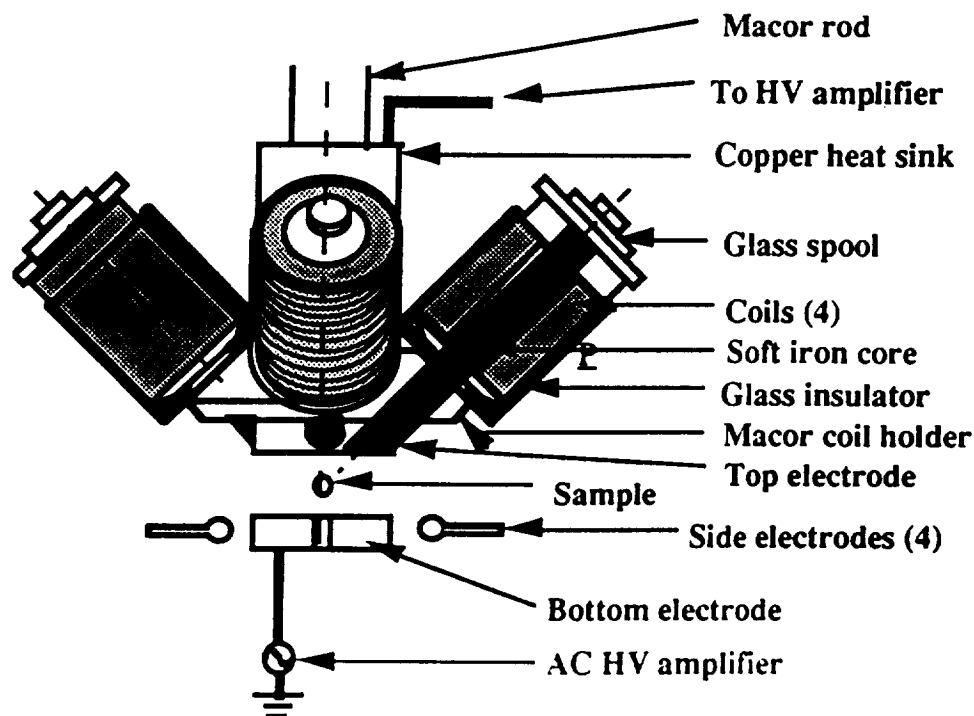

Fig. 1. A schematic of the electrode assembly.

charged sample to cancel the downward gravitational force. The four small side electrodes located around the bottom electrode control the sample position along the horizontal directions. The main position control voltage is connected to the upper electrode, while the bottom

4

electrode is electrically grounded through an AC voltage source. This AC voltage source generates oscillating electric field on the drop for the purpose of inducing resonant oscillations. To induce a sample rotation, a four-coil system was mounted on the top electrode. These coils produce a horizontal magnetic field that rotates at an appropriate frequency (400 Hz in the present experiment). The electrode assembly was housed by a stainless steel chamber which was typically evacuated to $\sim10^{-8}$ torr. Samples were heated using an xenon arc lamp. A detailed description of the HTESL was given in an earlier publication[9].

Experiments were conducted using a high purity aluminum and tin samples at approximately 25 K above the respective melting points. Initially, the resonance oscillation of n=2 mode was measured on a non-rotating drop by applying a low-level AC field. Subsequently the AC field was turned off, and the sample rotation was initiated by applying a rotating magnetic field at a preset amplitude and frequency.

The basic principle of the present sample rotation mechanism is essentially the same as asynchronous induction motor. The four-coil assembly works as a stator while the levitated sample serves as a rotor. According to the principle of the induction motor[10, 11], if an AC voltage E_1 at frequency ω_s is applied to a stator having a resistance R_1 and an inductance L_1, the torque τ experienced by the rotor (having its own resistance R_2 and inductance L_2) rotating at an instantaneous rotation frequency ω is given by

$$\tau = \frac{\omega_s E_1^2}{R_1^2 + \omega_s^2 L_1^2}\left(\frac{sR_2}{R_2^2 + s^2 L_2^2}\right),$$ (1)

where

$$s \equiv \frac{\omega_s - \omega}{\omega_s}.$$ (2)

Eq. (1) was tested using a levitated aluminum sphere by measuring the torque for given input parameters as a function of sample rotation frequency. Fig. 2 shows that at a fixed stator current the torque is a linear function of s, i.e. to the instantaneous sample rotational frequency.

This means that the relationship $R_2^2 \gg s^2L^2$ is well satisfied in Eq. (1), transforming Eq. (1) to a simpler form:

$$\tau = (\frac{\omega_s E_1^2}{R_1^2 + \omega_s^2 L_1^2})\frac{1}{R_2}(1 - \frac{\omega}{\omega_s}).$$ (3)
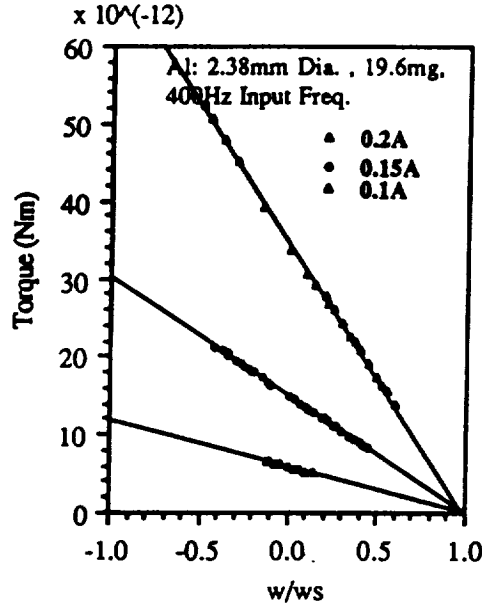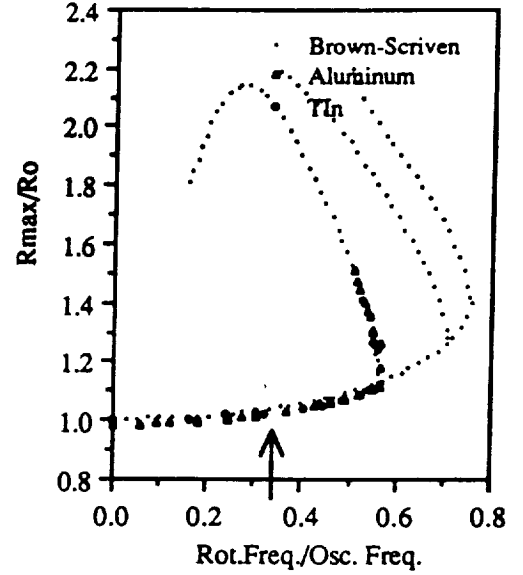

Fig. 2. Torque vs. sample rotation frequency.

Fig. 3. Drop shape vs. rotation frequency.

Accurate measurements of sample rotation frequency were important for the determination of torque imparted to the sample. In our experiment, a He-Ne laser beam was directed to the sample, and the reflected beam was detected by a silicon photo-detector. The output voltage of the detector was amplified and digitized to get a Fourier power spectrum, using a micro-computer. Such a power spectrum showed peaks at all harmonics of the sample rotation frequency. Such power spectrum only serves as a coarse indicator of the rotation frequency. More precise detection of sample rotation was done by exploiting the strobing effect created by a TV monitor. Regular monitors have 30-Hz frame rate (or 60-Hz field rate). A CCD camera operated at the shutter speed 0.001 second was mounted on a tele-microscope to produce a magnified sample image on a TV screen. Whenever the sample rotation rate

6

approached one of the harmonic or sub harmonic frequencies of the 60-Hz field rate, a seemingly static image appeared on the screen. Such a stroboscopic approach assisted by the power spectrum display allowed a precise determination of sample rotation frequency without ambiguity.

3. Experiment on Solid Body Rotation.

For drop rotation experiments, we chose a high purity aluminum and a tin sample. All parameters relevant to these samples and experimental conditions are shown in Table I. Each rotation experiment was initiated by applying a rotating magnetic field to the sample and by video-recording the side view of the drop. Drop rotation frequency was also overlaid on the video images.

As the drops started rotating, the nearly spherical initial shape progressively turned into a oblate spheroidal shape, and this trend continued until they reached a critical point, the bifurcation point, at which the axisymmetric shape became unstable and it turned into a triaxial ellipsoidal shape. As the drop gained angular momentum , the drop rotation frequency started to decrease even though the drop gained more angular momentum as a result of rapidly increasing moment of inertia. This behavior is in accordance with the earlier ground-based experimental results on rotating charged water drops[4] as well as with the experiments on uncharged drops conducted by Wang et al.[7] in a micro-gravity condition.

Fig. 3 shows the evolution of a normalized drop dimension, R_{max}/R_0, versus the normalized rotation frequency, $\omega_{rot}/\omega_{osc}$, where R_{max} and R_0 are the maximum radius of the rotating drop and the radius of spherical shape, respectively. The drop rotation frequency ω_{rot}. is normalized by its own oscillation frequency ω_{osc} (n = 2 mode) measured at the non-rotating state. Also plotted in Fig.3 is the theoretical results calculated by Brown and Scriven[3] showing an initially axi-symmetric drop shape branching out to a two-lobed, three-lobed, or four-lobed drop shape at certain critical frequencies. In reality, however, the two-lobed branch was the one to which the shape transformation from axisymmetric shape took place. Transition

between these two branches was reversible as long as the applied torque level was kept sufficiently low to ensure solid body rotation. Fig. 3 shows that the experimental points of both the aluminum and tin drops followed the theoretical curve within 2%. We observe that the data points along the axi-symmetric branch are slightly below the theoretical curve. This was caused due to the slightly oblate spherical shape of the drop in initially non-rotating state. The observed bifurcation point also agrees with the predicted value, $\omega_{rot}/\omega_{osc} = 0.559$, within 2%.

4. An anomaly Observed in Rotating Tin Drops

An anomalous behavior was observed when a rotating experiment was performed with a molten tin drop (39.8 mg). When the drop was rotated at a high torque level, the data points overshot the predicted bifurcation point (see Fig. 4). The drop angular momentum was further increased to a point where R_{max}/R_0 was approximately 1.6. Applied torque was turned off at this point, allowing the drop to rotate freely (in the frictionless vacuum) for the next two hours at the same temperature. Now, when the drop angular momentum was slowly reduced under the influence of negative torque, surprisingly the drop shape evolved following quite a different path away from the theoretical branches. In fact, the drop shape remained as triaxial ellipsoidal all the way down to the non-rotating state, completely by-passing the axi-symmetric branch. When the rotation frequency was slowed down to approximately 10 Hz, the drop (originally with its longest axis perpendicular to the vertical rotation axis) became unstable, and it eventually aligned its longest axis along the gravity field as the angular momentum was further reduced. The cause of this anomaly is not understood at this moment. Present authors only speculate that the probable cause might be isotopes in the rotating tin drop separating under the influence of centrifugal force, although we failed to confirm this using the Secondary Ion Mass Spectrometer. Tin has seven highly abundant isotopes between [116]Sn (14.53%) and [124]Sn (5.79%), among which [120]Sn (32.59%) is the most abundant isotope. The similar anomaly was not observable in rotating molten aluminum drops. This is probably due to the fact that [27]Al has essentially only one naturally abundant isotope. If we consider a sphere, 1.5 mm in

radius, that is rotating at 50-Hz, the difference in centrifugal acceleration between the center and the surface of the drop is as much as 15 times the Earth's gravitational acceleration. More systematic experiments and theoretical modelings may be required to understand this phenomena.
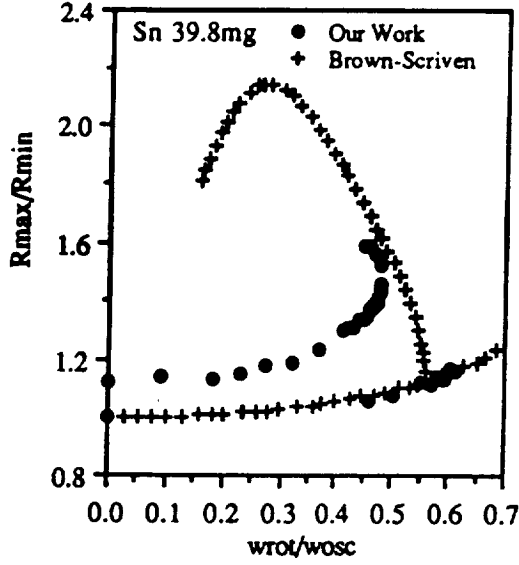

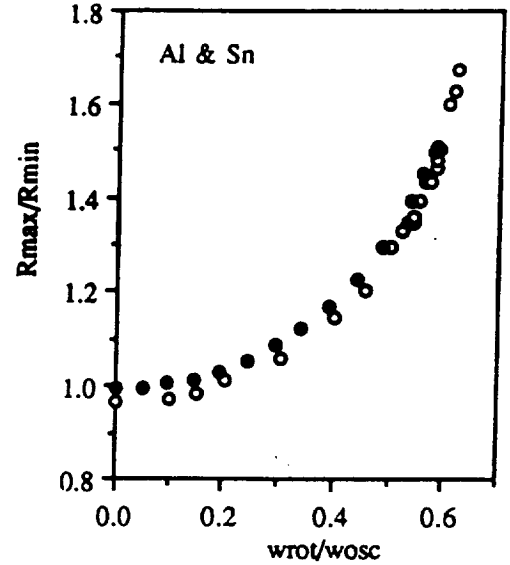Fig. 4. An anomaly in rotating tin drop.

Fig. 5. Drop shapes of Al and Sn vs. rot. freq.

5. A New Approach to Surface Tension Measurement

In this section the possibility of measuring the liquid surface tension from a rotating drop will be investigated. For low viscosity liquids, the drop oscillation detection is an accurate non-contact method of measuring the surface tension of a levitated drop[8]. However, for highly viscous liquids where resonant oscillations cannot be induced, a different non-contact method was needed to measure the surface tension.

If a drop rotates according to the theoretical curve as shown in Fig.3, one can determine the oscillation frequency, ω_{osc}, at any point of the curve, if the shape parameters, R_{max}/R_0 and the rotation frequency ω_{rot}, are known. We note that the liquid viscosity does not play any role in the theory of rotating drops as long as the drop can reach the condition of solid-body rotation. Higher viscosity will only help to bring the solid-body condition quickly. This

9

proposal of measuring the surface tension based on the drop rotation was first made by Elleman et al.[12]. Since the drop rotation frequency of an axi-symmetric drop is difficult to measure if the drop surface is extremely uniform, the drop rotation frequency should be made on the triaxial branch close to the bifurcation point. Since $\omega_{rot}/\omega_{osc} = 0.559$ at the bifurcation point, ω_{osc} can determined if ω_{rot}.is measured. This approach for the surface tension measurement should be applicable to homogeneous liquids regardless of their viscosities as long as the solid-body rotation condition is obeyed.

In this section, we intend to verify this alternative approach to the measurement of surface tension using a molten tin and an aluminum drops. Since both drops showed surface structures due to oxide layers, utilizing such oxide patches as tracers, the drop rotation along the axi-symmetric branch could be followed accurately. To obtain a more amplified view of drop shape changes, the axi-symmetric values of the two rotating melts and the theoretical points were plotted in terms of the ratio between the maxmum (or horizontal) and the minimun (or vertical) dimensions of the drop R_{max}/R_{min} as shown in Fig.5. When they were static (i.e. $\omega_{rot} = 0$), both drops showed slight elongation along the vertical direction. If appropriate multiplication factors which would make $R_{max}/R_{min} = 1$ at $\omega_{rot}/\omega_{osc} = 0$ are found and used them to normalize other data points in each set of data, the agreement of both of the normalized data with the theory was very good, and the fitting curve to the data could be expressed by

$$R_{max}/R_{min} = 1 - 6.655 \times 10^{-2} F + 1.663 F^2 - 2.669 F^3 + 4.445 F^4, \qquad (4)$$

where $F=\omega_{rot}/\omega_{osc}$. This equation can be used to determine $F=\omega_{rot}/\omega_{osc}$ for a given R_{max}/R_{min}. Since ω_{rot} can be measured ω_{osc} is determined. This procedure was applied to a rotating molten tin in order to demonstrated the validity of the new method of measuring the surface. Fig. 6 shows the effective oscillation frequency, $\omega_{osc}/2\pi$, as a function of normalized rotation frequency. For the comparison, Fig. 6 also shows the actual oscillation frequency that was measured at the same temperature. At the lower rotation frequency, the effective oscillation

frequency scattered widely, then, it rapidly converged to the actual oscillation frequency as the drop rotation frequency approached the bifurcation point, i.e. $\omega_{rot}/\omega_{osc} = 0.559$. This can be
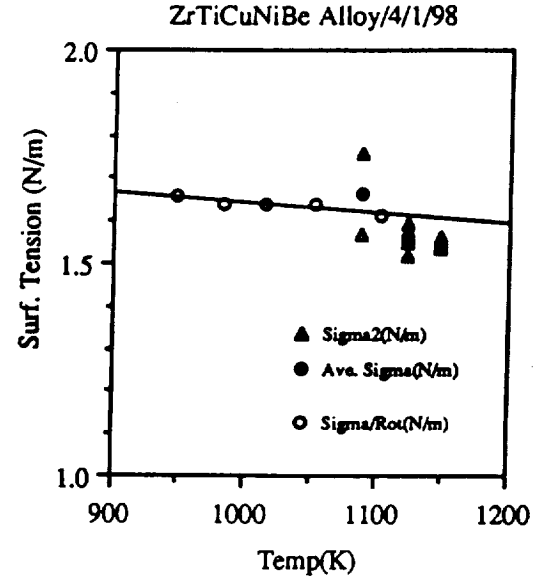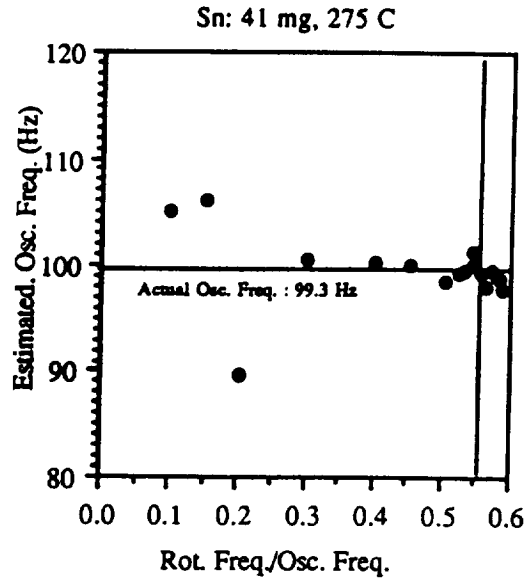
Fig. 6. Effective oscillation frequency vs. rot. freq.   Fig. 7. Surface tension of a glassforming alloy ($Zr_{41.2}Ti_{13.8}Cu_{12.5}Ni_{10.0}Be_{22.5}$). The triangles are the data taken by the oscillation method, and the solid circles show the averages of these data. The open circles are the surface tensions measured using the rotation based technique.

understood since R_{max}/R_{min} increases rapidly as the rotation frequency increases (see Fig. 5), thus, giving higher accuracy in $\omega_{rot}/\omega_{osc}$ when it was determined from a rapidly rotating state. From the figure one can see the effective oscillation frequency agreed with the actual frequency within ± 2 % (which corresponded to ± 2 Hz). This accuracy is lower than that of directly measured oscillation frequency that was reproducible within 0.5 Hz of accuracy. However, the fact that this non-contact technique can measure the surface tensions of highly viscous liquids makes it unique in itself. Furthermore, it is believed that the accuracy of the effective frequency may be increased if more accurat measurement of drop dimensions can be made.

Under the assumption of a uniform distribution of surface charge, ω_{osc} so obtained is related to the surface tension of the liquid σ by[13]

$$\omega_{osc.}^2 = \frac{8\sigma}{\rho r_\bullet^3}(1 - \frac{Q_s^2}{64\pi^2 r_\bullet^3 \sigma \varepsilon_\bullet}), \tag{5}$$

where ρ is the liquid density, r_0 is the radius of the static spherical drop, and ε_0 is the permitivity of the vacuum. The surface charge Q_s can be determined from the levitation condition between two flat parallel electrodes:

$$mg = \frac{Q_s V}{L}, \tag{6}$$

where m is the sample mass, g is the gravitational acceleration, V is the potential difference between the electrodes, and L is the spacing between electrodes. Strictly speaking, the shape of a drop which is levitated by an electric force against the gravity deviates from a perfect sphere, and the surface charges are not distributed uniformly. Oscillation of an electrostatically levitated drop in such a non-ideal situation has been examined recently by Feng and Beard[14], using the multiple parameter perturbation method. Their frequency correction term for axisymmetric n=2 mode is given by

$$\omega_{2c+}^2 = \omega_{osc.}^2[1 - F(\sigma, q, e)], \tag{7}$$

where ω_{2c+} is the measured frequency, ω_{osc} is defined by Eq. (5), and q and e are defined by

$$q^2 \equiv \frac{Q_s^2}{16\pi^2 r_\bullet^3 \varepsilon_\bullet}, \tag{8}$$

and $\qquad e^2 \equiv E^2 r_\bullet \varepsilon_\bullet,$ $\qquad\qquad\qquad\qquad$ (9)

respectively, where E is the applied electric field. $F(\sigma, q, e)$ in Eq. (7) is defined by

$$F(\sigma,q,e) \equiv \frac{(243.31\sigma^2 - 63.14q^2\sigma + 1.54q^4)e^2}{176\sigma^3 - 120q^2\sigma^2 + 27\sigma q^4 - 2q^6}.\tag{10}$$

This new technique for surface tension measurement was applied to a bulk glassforming alloy $(Zr_{41.2}Ti_{13.8}Cu_{12.5}Ni_{10.0}Be_{22.5})$. This alloy had such a high viscosity that the drop oscillations could not be induced below 1080K $(T_m=993K)$. For low viscosity liquids, the drop oscillation technique[8] is an adequate non-contact technique for the surface tension measurement. However, for high viscosity liquids where drop oscillations cannot be induced, the new non-contact technique for surface tension has to be applied. For example, viscosities of glass forming alloy liquids increase nearly 14 orders magnitude as they approach their glass transition temperatures. Fig. 7 shows the surface tensions of the glassforming alloy that were measured with the new technique. I also shows the surface tension data that were obtained using the drop oscillation technique. The open circles are the surface tensions measured using the rotation based technique (or the drop rotation method). The triangles are the data taken by the oscillation method and the solid circles are the averages of these data. One can observe in Fig. 7 that the drop oscillation method turned out to be less accurate showing increased scatter as the sample temperature was lowered.

6. Oscillation of Rotating Drop

Utilizing the systematic drop rotation capability, an attemp was made to verify the Busse's prediction[15] using a molten metallic drop although it was already verified by Annamali et al.[16] who used a acoustically suspended oil drop in a water tank. A molten aluminum drop was rotated along the virtical direction and the axi-symmetric mode of oscillations, i.e. $P_2(\cos\theta)$-mode, was induced at a given rotation frequency. Fig. 8 shows a good agreement between our experimental results and the Busse's theoretical prediction. This demonstration again emphasizes the effect of drop rotation on the measured drop oscillation

13

frequency. Put it differently, the measured drop oscillation frequency may be lead to a quite wrong surface tension if the state of drop rotation is ignored or unaccounted for.
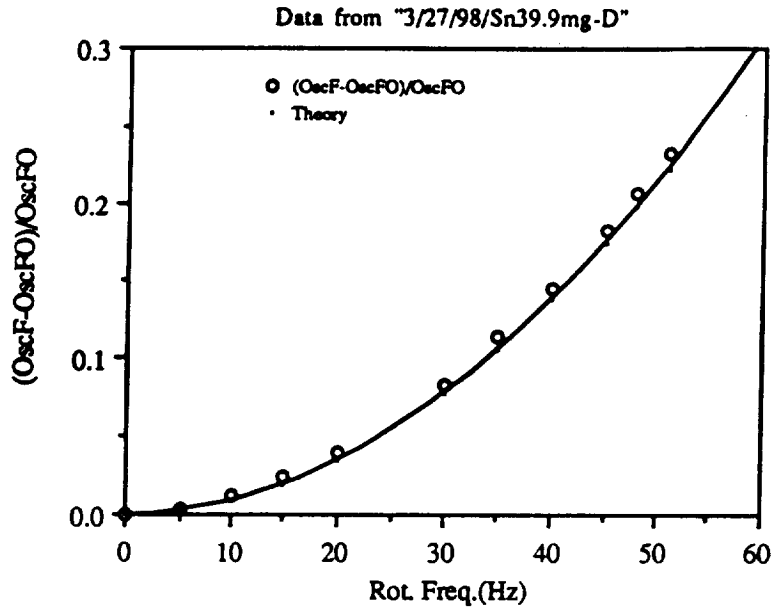

Fig. 8. Normalized oscillation frequncy measured as a function of rotation frequency of a molten aluminum was compared with the theory by Busse.

6. Summary and Discussions

A new technique, capable of systematically inducing rotation on a levitated metallic drop, was used for the study of dynamics of rotating charged drops. Although the drops carried surface charges, the experimental results showed close agreement with the Brown & Scriven's theory. This experiment showed that the surface charge on the drops (although aluminum had 24%, and tin had as much as 41% of their respective Rayleigh charge limits) did not cause any deviation from the prediction. These results are consistent with the previous results obtained from rotating charged water drops[4]. Good agreement with the prediction was possible only when the condition of solid-body rotation was abided. Under the influence of high level torque, the bifurcation of drop shape did not occur at the predicted point. Instead, the

data points overshot the axi-symmetric branch beyond the bifurcation point before it transformed into the two-lobed branch.

An anomalous behavior was observed in a rotating tin drop which showed a strong deviation from the prediction. We speculated that this anomaly was caused by isotope separation under the influence of the centrifugal force that was as strong as 15-g.

Based on the drop rotation capability, an alternate approach to the surface tension measurement was demonstrated. The effective oscillation frequency obtained from the rotation experiment near the bifurcation point agreed with the actual oscillation frequency within ±2%. This is an encouraging result in view of the fact that we now have a non-contact method of measuring surface tension of viscous liquids where the drop oscillation method cannot be applied. This technique was successfully applied to measure the surface tension of a highly viscous liquid, a bulk glassforming alloy $Zr_{41.2}Ti_{13.8}Cu_{12.5}Ni_{10.0}Be_{22.5}$ in its undercooled state.

The influence of the drop rotation on the drop oscillation was demonstrated verifying the Busse's theoretical prediction. This experiment will also serve as a warning toward the surface tension measurements, i.e. the drop rotational state has to be always monitored when the drop oscillatioin method is used for the determination of surface tension.

References:

[1 Lord Rayleigh, Phil. Mag. 28, 161, 1914.

[2] S. Chandrasekhar, "The Stability of a Rotating Liquid Drop," Proc. Roy. Soc. London, A 286, 1, 1965.

[3] R. A. Brown and L. E. Scriven, "The Shape and Stability of Rotating Liquid Drops," Proc. R. Soc. Lond. A 371, 331, 1980.

[4] W-K. Rhim, S.K. Chung, and D.D. Elleman, "Experiments on Rotating Charged Liquid Drops," Proc. 3rd International Colloquium on Drops and Bubbles (ed. T. G. Wang), AIP Conf. Proc. 197: 91, 1988 .

[5] A. Biswas, E. W. Leung, and E. H. Trinh: "Rotation of ultrasonically levitated glycerol drops", J. Acoust. Soc. Am. 90, 1502-1507, 1991.

[6] T. G. Wang, E. H. Trinh, A. P. Croonquist, and D. D. Elleman, "Shapes of Rotating Free Drops: Spacelab Experimental Results," Phys. Rev. Let. 56, 452, 1986.

[7] [11] T. G. Wang, A. V. Anilkumar, C. P. Lee and K. C. Lin: "Bifurcation of rotating liquid drops: results from USML-1 experiments in Space", J. Fluid Mech. 276, 389-403, 1994.

[8] W. K. Rhim, K. Ohsaka, P-F. Paradis and R. E. Spjut, "A non-contact technique of measuring surface tension and viscosity of molten materials using high temperature electrostatic levitation", Rev. Sci. Instrum. (in press)

[9] W. K. Rhim, S. K. Chung, D. Barber, K. F. Man, G. Gutt, A. Rulison, and R. E. Spjut, "An Electrostatic Levitator for High Temperature Containerless Materials Processing in 1-g," Rev. Sci. Instrum. 64: 2961, 1993.

[10] S. A. Nasar and I. Boldea, Electric Machines (Steady tate Operation), Hemisphere Publishing Corporation, 1990.

[11] P. L. Alger, Nature of Induction Machine, Gordon and Breach Science Publishers, 1965.

[12] D. D. Elleman, T. G. Wang, and M. Barmatz, "Acoustic Containerless

Experiment System: A Non-Contact Surface Tension Measurement," NASA Tech. Memo. 4069, Vol. 2, 557, 1988.

[13] Lord Rayleigh, Phil. Mag. "On the Equilibrium of Liquid Conducting Masses Charged with Electricity," 14, 184, 1882.

[14] Q. Feng and K. V. Beard: Proc. Roy. Soc. Lond. A. 430, 133, 1990

[15] F. H. Busse: "Oscillations of a rotating liquid drop", J. Fluid Mech. 142, 1-8, 1984.

[16] P. Annamalai, E. T. Trinh, and T. G. Wang, "Experimental Studies of the Oscillation of a Rotating Drop," J. Fluid Mechs., 158, 317, 1985.

Table I: Parameters relevant to samples used to obtain the data shown in Fig. 3.

Samples	Aluminum	Tin
Weight (mg)	26.5	27.1
Melting Point T_m (°C)	660.5	232
Sample Temperature (°C)	705	320
Density at T_m (g/cm^3)	2.38	6.98
Surf. Tension at T_m (mN/m)	914	560
Viscosity at T_m (mP·sec)	2	1.81
Net Electric Charge (nCoul.)	0.445	0.3451
Rayleigh Limit (nCoul.)	1.843	0.851
$Q/Q_{Rayleigh}$ (%)	24.16	41.2